Structural Requirements of MLD-Containing Disintegrins for Functional Interaction with α4β1 and α9β1 Integrins

Stanislawa Bazan-Socha,[‡] Dariusz G. Kisiel,[‡] Brad Young,[§] R. David G. Theakston,[||] Juan J. Calvete,[⊥] Dean Sheppard,[§] and Cezary Marcinkiewicz*,[‡]

Department of Biology, College of Science and Technology, Temple University, Philadelphia, Pennsylvania 19122, Lung Biology Center, Department of Medicine, University of California, San Francisco, CA 94110, Alistair Reid Venom Research Unit, Liverpool School of Tropical Medicine, Pembroke Place, Liverpool L3 5QA, U.K., and Instituto de Biomedicina de Valencia, CSIC, E-46010 Valencia, Spain

Received October 14, 2003; Revised Manuscript Received December 8, 2003

ABSTRACT: Three non-RGD-containing disintegrins, VLO5, EO5, and EC3, belong to the hetrodimeric family of these snake venom-derived proteins. They are potent inhibitors of certain leukocyte integrins such as α4β1, α4β7, and α9β1, and act through the MLD motif present in one of their subunits. However, the selectivity of these disintegrins to interact with integrins is related to the amino acid composition of the integrin-binding loop in the MLD-containing subunit. The most important amino acid is that preceding the MLD motif. In vitro experiments in adhesion and ELISA assays revealed that the TMLD-containing disintegrins, VLO5 and EO5, appeared to be very potent inhibitors of human α4β1 and α9β1 and less effective in inhibition of the α4β7 integrin. The reverse effect was observed for the AMLD-containing disintegrin, EC3. The data with native disintegrins were confirmed by experiments with synthetic peptides displaying TMLD and AMLD motifs. The MLD-containing disintegrins showed differential activities to inhibit human and murine α4β1 integrin. EC3 was a weaker inhibitor of human integrin, whereas VLO5 and EO5 less actively inhibited murine α4β1. These data describe a useful set of potent and selective integrin antagonists and suggest conformational requirements of human and mouse integrins for interaction with ligands.

Integrins are the large family of adhesion receptors broadly expressed on all cell types. The interactions of integrins with extracellular matrix proteins and cell adhesion molecules are important events in organ physiology, as well as in the pathology of many diseases (*1*−*4*). Structurally, integrins are type I transmembrane glycoproteins composed of noncovalently linked α and β subunits. Currently, 18 α and 8 β subunits have been identified on the surfaces of human cells. These subunits are combined in a restricted manner to form at least 24 heterodimeric assemblies, each exhibiting a distinct ligand-binding profile (*3*, *4*). Integrin-mediated adhesion is a tightly regulated bidirectional signaling process, which integrates the intracellular and the extracellular environments (*5*−*7*). Cytoplasmic interactions between the integrin subunits result in the transmission of conformational changes through the membrane-spanning regions that regulate the affinity of the integrin extracellular domains (*8*).

Integrins expressed on the leukocytes play a significant role in the development of the inflammatory response; the most important integrins involved in leukocyte invasion are β2 integrins and certain β1 integrins. These interact with adhesion molecules expressed on cytokine-activated, vascular endothelium. Thus, integrins are potential targets for treatment of immune-mediated diseases, such as rheumatoid arthritis, multiple sclerosis, insulin-dependent diabetes mellitus, and asthma (*9*, *10*).

The α4β1 and α9β1 integrins expressed on T-cells and neutrophils are recognized as receptors for vascular cell adhesion molecule 1 (VCAM-1[1]). VCAM-1 belongs to the immunoglobulin superfamily and is expressed on the endothelial cells at sites of inflammation (*11*, *12*). α4β1 also binds to alternatively spliced variants of fibronectin that contain connective segment 1 (CS-1). The binding motif in the CS-1 fragment has been identified as LDV tripeptide (*13*), whereas in VCAM-1 it is IDSP tetrapeptide (*14*). The α4 and α9 subunits are structurally related. However, many other distinct ligands have been identified for α9β1, including tenascin-C (*15*) and osteopontin (*16*). The binding site of α9β1 on tenascin-C has been identified as the AEIDGIEL sequence (*17*), whereas on osteopontin it is the SVVYGLR sequence immediately adjacent to the RGD site (*18*).

Disintegrins are low molecular weight proteins isolated from the venom of many species of vipers (*19*−*24*). They

* To whom correspondence should be addressed. Phone: (215) 707-4419. Fax: (215) 707-2783. E-mail: cmarcink@temple.edu.
[‡] Temple University.
[§] University of California.
[||] Liverpool School of Tropical Medicine.
[⊥] CSIC.

[1] Abbreviations: BSA, bovine serum albumin; CHO, Chinese hamster ovary; CMFDA, 5-chloromethylfluorescein diacetate; HBSS, Hanks balanced salt solution; HPLC, high-performance liquid chromatography; MALDI-TOF-MS, matrix-assisted laser-desoption ionization time-of-flight mass spectrometry; MAdCAM-1, mucosal addressin cell adhesion molecule 1; PBS, phosphate-buffered saline; TFA, trifluoroacetic acid; VCAM-1, vascular cell adhesion molecule 1.

10.1021/bi035853t CCC: $27.50
Published on Web 01/21/2004

have a conserved pattern of cysteines, which are involved in the creation of intramolecular disulfide bonds for monomeric disintegrins. Conversely, in dimeric disintegrins, the disulfide bonds have been localized as intra- and intersubunit links between cysteines (*22*). The integrin-inhibitory activity of disintegrins critically depends on the appropriate pairing of cysteine residues, which determines the conformation of the inhibitory loop. Monomeric disintegrins, initially described as potent inhibitors of the platelet αIIbβ3 fibrinogen receptor, are frequently inhibitors of other RGD-dependent integrins, including αvβ3 and α5β1 (*23*, *24*). In most single-chain disintegrins the active sequence is the tripeptide RGD (*21*). Exceptions are barbourin and ussuristatin 2, possessing an active KGD sequence (*25*, *26*) and atrolysin E, which has an MVD motif in its inhibitory loop (*27*). These disintegrins also exhibit potent inhibitory activity against the platelet αIIbβ3 integrin. Monomeric disintegrins show different levels of affinity and selectivity toward the αIIbβ3, αvβ3, and α5β1 integrins, which strongly depend on amino acids adjacent to the RGD motif within their integrin-binding loops (*23*, *24*, *28*).

Heterodimeric disintegrins exhibit more variability of the amino acid sequences of their active sites (*29*). Some have RGD sequences in both subunits (*30*), whereas in others the corresponding sequence in one subunit may be MGD (*31*), KGD (*32*), WGD (*33*), and MLD and VGD (*34*, *35*). The hypothesis has been put forward that the conserved aspartate residue might be responsible for the binding of disintegrins to integrin receptors which share a β subunit, while the two other residues of the integrin-binding motif (RG, KG, MG, WG, ML, VG) may dictate the integrin specificity (*29*). One interesting group is the MLD-containing disintegrins; two of these, EC3 and EC6, are potent inhibitors of α4 and α9β1 integrins (*34*, *35*). The biological activity of the MLD sequence has been confirmed by short peptide synthesis. Experiments in vivo with NOD (diabetic) mice have revealed that EC3 inhibited lymphocyte-dependent infiltration of Langerhans islets (*36*). Here we report two new MLD-containing, non-RGD-displaying heterodimeric disintegrins and demonstrate the importance of the amino acids surrounding this active motif for selective interaction with integrins.

EXPERIMENTAL PROCEDURES

Monoclonal Antibodies. Y9A2 against human α9β1 was prepared as described previously (*37*). AJH10 against the I-domain of the human α1 subunit of VLA-1 (38) was provided by Dr. R. Lobb (Biogen Inc., Cambridge, MA). HP2/1, P1E6, P1B5, and SAM-1 were purchased from Chemicon (Temecula, CA). Ha31/8, HMα2, clone 42, R1-2, HMα5-1, GoH3, and Ha2/5 were purchased from BD Pharmingen (San Diego, CA). Lia1/2 was purchased from Beckman Coulter Inc. (Fullerton, CA).

Integrin Ligands. The recombinant chicken tenascin-C fragment (TNfn3RAA) was generated from an expression plasmid obtained from Dr. K. Crossin (Scripps Research Institute, La Jolla, CA), and the recombinant N-terminal fragment of human osteopontin was acquired from Dr. Y. Yokasaki (Hiroshima University, Japan). Recombinant human VCAM-1/Ig and MAdCAM-1 were obtained from Dr. R. Lobb (Biogen), and recombinant mouse VCAM-1/Ig was donated by Dr. M. Renz (Genentech, San Francisco, CA). Highly purified fibrinogen was a gift from Dr. A. Budzynski (Temple University, Philadelphia, PA). Bovine collagen type I, collagen type IV, and human vitronectin were purchased from Chemicon, and human fibronectin and laminin were purchased from Sigma (St. Louis, MO).

Snake Venoms. The venoms of *Echis carinatus sochureki* and *Vipera* (=*Macrovipera*) *lebetina obtusa* were purchased from Latoxan Serpentarium (Valence, France). The venom of Nigerian *Echis ocellatus* was collected from the wild-caught specimens as described previously (*39*).

Cell Lines. α9- and mock-transfected SW480 cells were generated as described previously (*15*). A5 cells, Chinese hamster ovary (CHO) cells transfected with human αIIbβ3 integrin (*40*), were kindly provided by Dr. M. Ginsberg (Scripps Research Institute). JY cells expressing αvβ3 were a gift from Dr. Burakoff (Dana Farber Cancer Institute, Boston, MA). K562 cells transfected with α1, α2, and α6 integrins were provided by Dr. M. Hemler (Dana Farber Cancer Institute, Boston, MA). The RPMI 8866 cell line was a gift from Dr. A. Garcia-Pardo (Centro de Investigaciones Biologicas, CSIC, Madrid, Spain). K562, Jurkat, Ramos, SW480, and human (HS.939T) and mouse (B16F10) melanoma cell lines were purchased from ATCC (Manassas, VA).

Purification of MLD-Containing Disintegrins. Lyophilized venoms were dissolved in 0.1% TFA (30 mg/mL). Insoluble material was discarded after centrifugation at 5000 rpm for 5 min, and the supernatant was fractionated by reversed-phase HPLC on a C18 (250 × 10 mm) column from Vydac (Hesperia, CA). The column was eluted with linear acetonitrile gradient 0−80% over 45 min at a flow rate of 2 mL/min. Separations were monitored at 206 nm, and fractions were collected manually and lyophilized using a Speed-Vac system. Lyophilized fractions were dissolved in water, and protein concentrations were determined using the BCA assay (Pierce, Rockfort, IL). Each fraction (5 μg of protein per well) was immobilized on 96-well microtiter plates (Falcon, Pittsburgh, PA) in PBS, overnight at 4 °C, and tested for its ability to support K562 cell adhesion (as described below). Fractions with adhesive properties were tested for their inhibitory effect on the adhesion of Jurkat cell adhesion to immobilized VCAM-1. Active fractions were rechromatographed using the same HPLC system but developing the column with a shallow gradient (0−60% B over 45 min). The purity of isolated MLD-containing, heterodimeric disintegrins was assessed by SDS−polyacrylamide gel electrophoresis and matrix-assisted laser-desoption ionization time-of-flight mass spectrometry (MALDI-TOF-MS) performed at the Wistar Mass Spectrometry Facility (Philadelphia, PA) using a PE-Biosystems Voyager-DE Pro instrument.

Isolation and Structural Characterization of Ethylpyridylated Subunits. Heterodimeric disintegrins VLO5 and EO5 (0.5 mg/mL in 0.1 M Tris−HCl, pH 8.5, 4 mM EDTA, 6 M guanidine hydrochloride) were reduced with 3.2 mM dithiothreitol for 2 h at room temperature in the dark. Reduced proteins were alkylated by addition of a 2-fold molar excess of 4-vinylpyridine over the reducing reagent. Ethylpyridylated (EP) subunits were isolated by reversed-phase HPLC on a C-18 column developed with a linear gradient of 0.1% TFA in water (solution A) and 0.1% TFA in acetonitrile (solution B), and were denoted "A" or "B" according to their

elution order. The isolated EP-subunits were initially characterized by N-terminal sequencing (using either an Applied Biosystems 477A or a Beckman Porton LF-3000 instrument following the manufacturer's instructions), amino acid analysis (using a Beckman Gold amino acid analyzer after sample hydrolysis in 6 M HCl for 24 h in evacuated and sealed ampules), and MALDI-TOF mass spectrometry (as above). The primary structures of EP-polypeptides were deduced from the N-terminal sequence analysis of overlapping peptides obtained by proteolytic digestions with TPCK-trypsin (Sigma), endoproteinase Lys-C (Boehringer Mannheim), and endoproteinase Asp-N (Boehringer Mannheim) (2 mg/mL protein in 100 mM ammonium bicarbonate, pH 8.3, for 18 h at 37 °C using an enzyme:substrate ratio of 1:100 (w/w)) and degradation with CNBr (10 mg/mL protein and 100 mg/mL CNBr in 70% (v/v) formic acid for 6 h at room temperature, under N_2 atmosphere and in the dark). Peptides were separated by reversed-phase HPLC using a 4 × 250 mm C18 (5 μm particle size) Lichrospher RP100 (Merck) column eluting at 1 mL/min with a linear gradient of 0.1% TFA in water (solution A) and 0.1% TFA in acetonitrile (solution B).

Purification of α9β1 and α4β1 Integrins. The isolation procedure of α9β1 and α4β1 was based on the method described previously for purification of recombinant αvβ3 integrin from transfected cells (*41*). However, the heterodimeric disintegrin VLO5 was used as a ligand coupled to the resin in the affinity column. VLO5 (20 mg per 2 mL of gel) was coupled to an Amino-Link Plus column (Pierce) according to the manufacturer's instructions. α9β1 and α4β1 integrins were purified from SW480 cells transfected with α9 integrin (*12*) and Ramos cell lines, respectively. About 2×10^8 α9SW480 cells or 5×10^8 Ramos cells were lysed in the presence of 10 mL of buffer containing 100 mM *n*-octyl glucoside, 50 mM Tris−HCl, pH 7.4, 150 mM NaCl, 1 mM $MgCl_2$, 1 mM $CaCl_2$, and 1 mM PMSF. After removal of insoluble material by centrifugation at 3000*g*, the extract was concentrated to 1 mL using Centriprep 10 (Millipore). The VLO5-agarose column (2 mL) was equilibrated with 50 mM Tris−HCl, pH 7.4, buffer containing 25 mM *n*-octyl glucoside, 150 mM NaCl, 2 mM $MgCl_2$, and 0.1 mM $CaCl_2$. The cell extract was applied to the column and incubated for 30 min at ambient temperature. The column was washed with the same buffer until protein disappeared from the eluate. It was then washed with the same buffer but with the concentration of NaCl increased to 300 mM. The integrin was eluted from the column by adding 15 mM EDTA to the buffer. Fractions (1 mL) were colleted in vials containing 30 μL of 1 M $MgCl_2$. The fractions interacting with Y9A2 mAb (α9β1) or HP2/1 mAb (α4β1) in ELISA assay were combined, concentrated to a volume of 1 mL (Centriprep 10), and dialyzed against Tris−HCl, pH 7.4, buffer containing 25 mM *n*-octyl glucoside, 150 mM NaCl, 1 mM $MgCl_2$, and 1 mM $CaCl_2$. The yields of the purified components were 50 and 30 μg for α9β1 and α4β1, respectively.

ELISA Assay. Plates containing 96 wells (BD Falcon, Franklin Lakes, NJ) were coated with purified α4β1 or α9β1 (5 μg/mL) overnight at 4 °C in PBS. The wells were blocked with 5% nonfat milk (BioRad, Hercules, CA) in PBS/Tween-20 (PBST) buffer. Increasing concentrations of disintegrins were added in Tris−HCl, pH 7.4, buffer containing 150 mM NaCl, 2 mM $MgCl_2$, 0.1 mM $CaCl_2$, and 1% BSA, and the plate was incubated for 30 min at 37 °C. After the plate was washed with the same buffer, human, recombinant VCAM-1/Ig was added at a concentration of 2 μg/mL. Incubation was continued for another 30 min at 37 °C. The bound VCAM-1/Ig was detected using goat antihuman IgG (Fc specific) conjugated with alkaline phosphatase (Sigma) as described previously (*36*).

Cell Adhesion Studies. Adhesion studies of cultured cells labeled with 5-(chloromethyl)fluorescein diacetate (CMFDA) were performed as described previously (*20*). Briefly, disintegrins, integrin ligands, or monoclonal antibodies were immobilized on a 96-well microtiter plate (BD Falcon) in PBS buffer overnight at 4 °C. Wells were blocked with 1% BSA in Hanks balanced salt solution (HBSS) containing calcium and magnesium. The cells were labeled with fluorescein by incubation at 37 °C for 15 min with 12.5 μM CMFDA in HBSS containing calcium and magnesium. Cells were freed from the unincorporated CMFDA label by washing with the same buffer. Labeled cells (1×10^5/sample) were added to the wells in the presence or absence of inhibitors and incubated at 37 °C for 30 min. Unbound cells were removed by aspiration, the wells were washed, and bound cells were lysed by adding 0.5% Triton X-100. The standard curve was prepared in parallel on the same plate using known concentrations of labeled cells. The wells were read using a Cytofluor 2350 fluorescence plate reader (Millipore, Bedford, MA) at an excitation wavelength of 485 nm using a 530 nm emission filter.

Peptide Synthesis. Peptides CKRTMLDGLNDYC and CKR**A**MLDGNDYC representing integrin-binding loops of VLO5 and EC3, respectively, were synthesized commercially at Sigma-Genosis (Woodland, TX).

RESULTS

Purification and Amino Acid Sequencing of MLD-Containing Disintegrins. Previously, we reported one non-RGD-containing, heterodimeric disintegrin, EC3, in which the active site was localized within the MLD sequence (*34*). This heterodimeric disintegrin was isolated from the venom of *E. carinatus sochureki* by two-step reversed-phase HPLC using a C18 column. Using the same method, we identified and purified two other non-RGD-containing, heterodimeric disintegrins, VLO5 and EO5, from the venoms of *V. lebetina obtusta* and *E. ocellatus*, respectively. Figure 1 compares the first step of purification of heterodimeric disintegrins EC3, VLO5, and EO5 as elution patterns of whole water-soluble proteins of viper venoms. The retention times for EC3, VLO5, and EO5 were 24, 25, and 24 min, respectively.

Fractions containing VLO5 and EO5 were collected and subjected to a second reversed-phase HPLC purification step as described in the Experimental Procedures. The purity of the isolated proteins was assessed by SDS−PAGE (Figure 1D), MALDI-TOF mass spectrometry, and N-terminal sequence analysis. Nonreduced VLO5 and EO5 migrated on SDS−PAGE as single bands with mobility similar to that of native EC3 (Figure 1D, lanes a−c) at apparent molecular masses of 15−20 kDa. However, under reduced conditions the subunits of VLO5 and EO5 were separated, whereas EC3 reduced subunits migrated with the same mobility. The molecular masses of the reduced subunits were decreased by ~50%, consistent with disulfide-linked dimers.

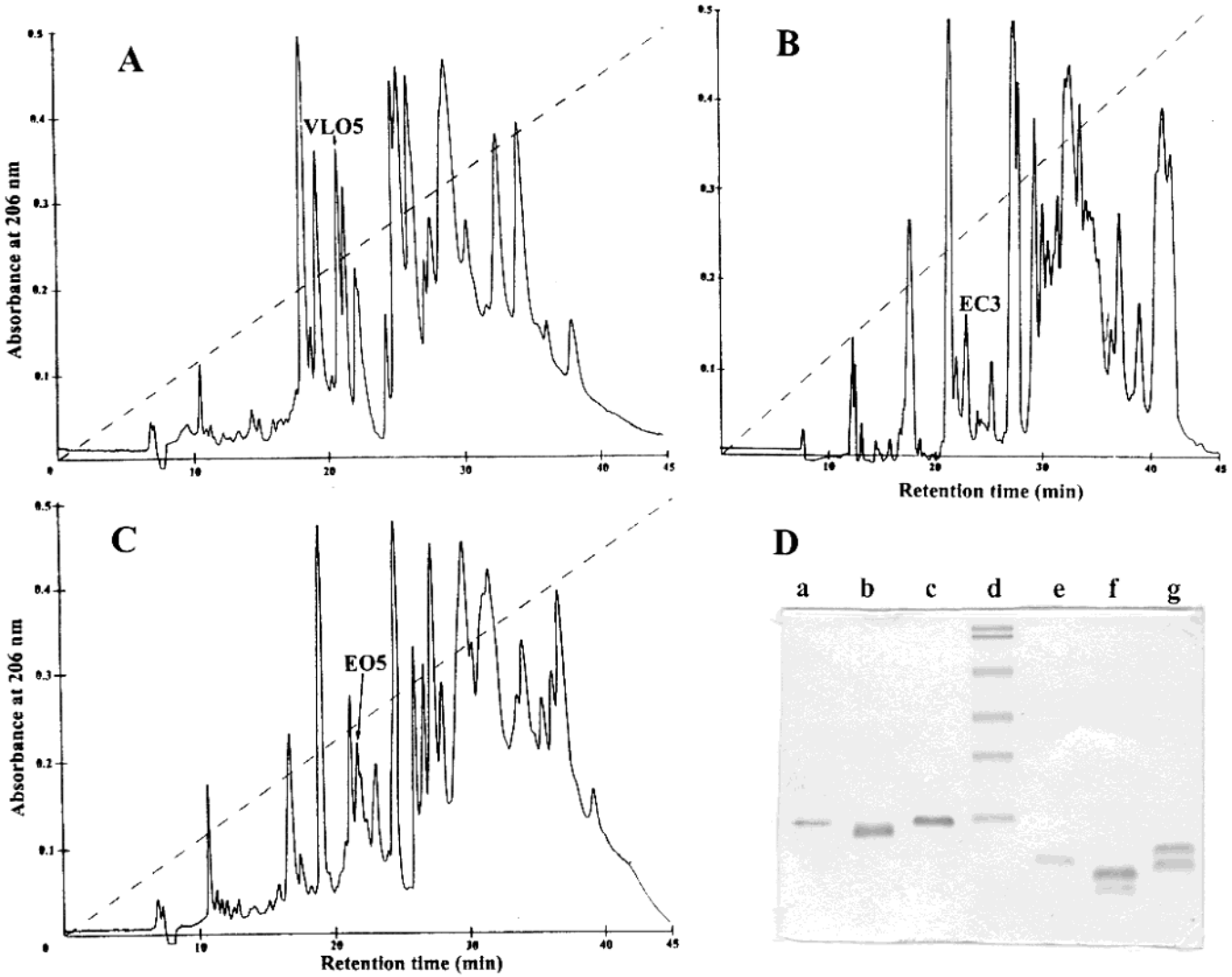

FIGURE 1: Purification of MLD-containing disintegrins on reversed-phase HPLC. The crude venoms of *V. (M.) lebetina obtusa* (A), *E. carinatus sochureki* (B), and *E. ocelatus* (C) were dissolved in 0.1% TFA and injected (10 mg in 400 μL) into a C18 column. Fractions separated with a 0−80% acetonitrile gradient (---) were collected and lyophilized. (D) SDS−PAGE (12.5% gel) of purified MLD-containing disintegrins: (a−c) EC3, VLO5, and EO5, respectively, in nonreduced gel; (e−g) EC3, VLO5, and EO5, respectively, in reduced gel; (d) molecular weight markers (Low Range Bio-Rad), 106, 77, 50.8, 35.6, 28.1, and 20.9 kDa.

MALDI-TOF mass spectrometric analysis of VLO5 and EO5 yielded single molecular ions of 14733 and 14514 Da, respectively. After reduction and alkylation with 4-vinylpyridine, both VLO5 and EO5 were resolved into two subunits, termed subunit A and subunit B according to their elution order, by reversed-phase HPLC. EP-VLO5A exhibited a single isotope-averaged molecular ion of 8163 Da, whereas EP-VLO5B yielded 8687 Da. On the other hand, EP-EO5A and EP-EO5B yielded ions at *m*/*z* 8456 and 8197 Da, respectively. Using the equation $N_{Cys} = (M_{PE} - M_{NAT})/106.3$, where N_{Cys} is the number of cysteine residues per molecule, M_{PE} is the mass of the reduced and pyridylethylated protein, M_{NAT} is the mass of the native, HPLC-isolated protein, and 106.3 is the mass increment due to the pyridylethylation of one thiol group, we calculated that native VLO5 and EO5 each contained 20 cysteine residues (N_{Cys}-(VLO5) = [(8163 + 8687) − 14733]/106.3 = 19.9; N_{Cys}-(EO5) = [(8456 + 8197) − 14514]/106.3 = 20.1).

The complete amino acid sequences of VLO5 and EO5 were established by N-terminal sequence analysis of sets of reversed-phase HPLC-purified overlapping fragments obtained by degradation of the PE-subunits. Figure 2 displays a comparison of the amino acid sequences of the VLO5 and EO5 subunits and the primary structures of the EC3 polypeptide chains. The large conservation of sequence characteristics, including the polypeptide lengths (VLO5A and VLO5B, 65 and 69 amino acids, respectively; EO5A and EO5B, 66 and 68 residues, respectively) and the conserved number and spacing of the 10 cysteine residues per subunit, clearly places VLO5 and EO5 in the group of snake venom heterodimeric disintegrins. Like EC3, VLO5 and EO5 possess MLD and VGD motifs in their integrin-recognition loops.

Biological Activities of MLD-Containing Disintegrins. The inhibitory activities of EC3, VLO5, and EO5 on a panel of human integrins were assessed using a cell adhesion assay (Table. 1). All three disintegrins proved to be potent inhibitors of $\alpha4\beta1$, $\alpha4\beta7$, and $\alpha9\beta1$ integrins. The disintegrins had a low inhibitory activity against two RGD-dependent integrins, $\alpha IIb\beta3$ and $\alpha5\beta1$. $\alpha v\beta3$, another RGD-dependent integrin, was not inhibited by these disintegrins up to a concentration of 10 μM. Likewise, there was no blocking of the collagen receptors $\alpha1\beta1$ and $\alpha2\beta1$ or the laminin receptor $\alpha6\beta1$. EC3, VLO5, and EO5 inhibit $\alpha4$,

EC3A
NSVHP**CC**DPVK**C**EPREGEH**C**ISGP**CC**RN**C**KFLRAGTV**C**KRA *VGD* DVDDY**C**SGITPD**C**PRNRYKGKED
EC3B
NSVHP**CC**DPVK**C**EPREGEH**C**ISGP**CC**RN**C**KFLNAGTI**C**KRA *MLD* GLNDY**C**TGKSSD**C**PRNRYKGKED

VLO5A
NSGNP**CC**DPVY**C**KPRRGEH**C**VSGP**CC**RN**C**KFLRAGTI**C**KRA *VGD* DMDDY**C**TGISSD**C**PRNPWKSE
VLO5B
MNSANP**CC**DPKT**C**KPRKGEH**C**VSGP**CC**RN**C**KFLSPGTI**C**KRT *MLD* GLNDY**C**TGVTSD**C**PRNPWKSEEED

EO5A
NSAHP**CC**DPVT**C**QPKKGEH**C**ISGP**CC**RN**C**KFLNSGTI**C**KKT *MLD* GLNDY**C**TGVTSD**C**PRNPYKGKEDD
EO5B
NSAHP**CC**DPVT**C**QPKKGEH**C**ISGP**CC**RN**C**KFLNSGTV**C**KRA *VGD* DMDDY**C**SGITTD**C**PRNPYKGKD

FIGURE 2: Comparison of amino acid sequences of EC3, VLO5, and EO5. Cysteine residues are in bold type. The integrin-binding motifs are shown in underlined italics.

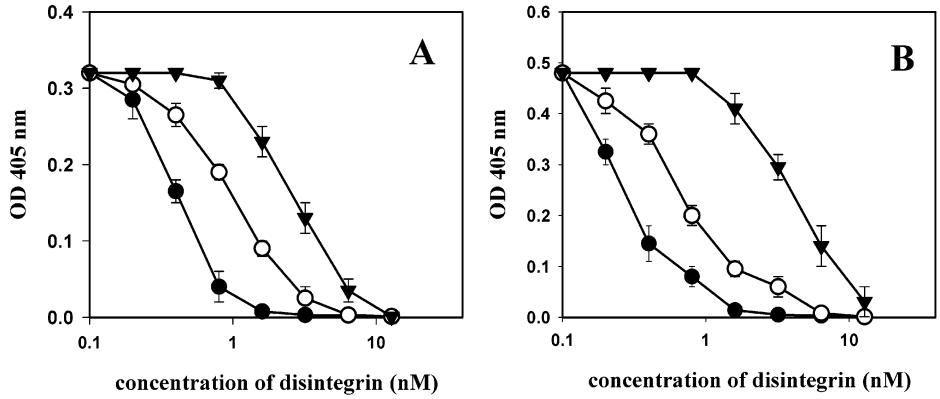

FIGURE 3: Effect of MLD-containing disintegrins on binding VCAM-1 to purified α4β1 (A) and α9β1 (B) integrins in ELISA assay. Purified human integrins (5 μg/mL) were immobilized on a 96-well plate. After blocking, increasing concentrations of VLO5 (filled circles), EO5 (open circles), or EC3 (filled triangles) were added to the wells and incubated for 30 min at 37 °C. The wells were then washed, recombinant VCAM-1 (2 μg/mL) was added, and incubation was continued for another 30 min at 37 °C. For detection of bound VCAM-1/Ig, goat antihuman IgG AP-conjugated was added and the plate was incubated for a further hour at 37 °C. The color was developed by AP substrate (pNPP), and the plate was read using an ELISA plate reader at a 405 nm single wavelength. The error bars represent the standard deviations from three independent experiments.

α9β1, αIIbβ3, and α5β1 integrins to different extents. VLO5 was the most selective inhibitor of α9β1 and α4β1 followed by EO5 and EC3. VLO5 potently inhibited adhesion of α9β1-expressing cells to three ligands, VCAM-1, tenascin-C, and osteopontin. On the other hand, EC3 did not inhibit adhesion to tenascin-C or osteopontin, but was more than 1 order of magnitude more active than VLO5 in inhibition of α5β1 adhesion to fibronectin. In contrast to inhibition of α4β1, VLO5 and EO5 were about 1 order of magnitude less active than EC3 in inhibiting α4β7 integrin binding to MAdCAM-1. A low potency of all three disintegrins against the fibrinogen receptor αIIbβ3 was also confirmed using the ADP-induced platelet aggregation assay. In this assay EC3, VLO5, and EO5 showed IC_{50} values of 1, 1.6, and 1.8 μM, respectively.

The activities of MLD-disintegrins against α4β1 and α9β1 were confirmed in an ELISA assay using purified integrins. The α4β1 and α9β1 integrins were purified from cultured cells, using a VLO5-Sepharose column. Ramos cells that naturally expressed α4β1 integrin were used as a source of α4β1, whereas the recombinant α9β1 was purified from SW480 cells previously transfected with α9. VLO5 and EO5 potently inhibited binding of VCAM-1 to immobilized α4β1, while the inhibitory effect of EC3 was lower (Figure 3A). The difference in activity of all three disintegrins was more striking in inhibition of purified VCAM-1 binding to immobilized α9β1 (Figure 3B). In agreement with the results of the adhesion assay, the inhibitory activity of VLO5 was almost 1 order of magnitude higher than that of EC3, whereas EO5 possessed intermediate activity.

Activity of Synthetic Peptides. Our earlier results showed that the anti-α4β1 activity of EC3 is related to the MLD sequence (*34*). VLO5 and EO5 display this sequence on their B and A subunits, respectively (Figure 2), suggesting functional association of these subunits with the activity of these two disintegrins. Although the MLD sequence is present in all of these disintegrins, VLO5 and EO5 are much more potent inhibitors of α4β1, and especially α9β1, than is EC3. On the other hand, EC3 is a more potent inhibitor of the RGD-dependent integrins α5β1 and αIIbβ3 (Table 1). It has been previously observed that this type of selective interaction with certain integrins among RGD-disintegrins depends on the amino acid adjacent to the RGD motif (*23*, *24*). A comparison of the amino acid composition of the MLD-loops of EC3 and VLO5 revealed only one difference in the position flanking the MLD motif from the N-terminus end; the alanine in EC3 is replaced by threonine in VLO5 (Figure 2). The activities of two synthetic, linear peptides

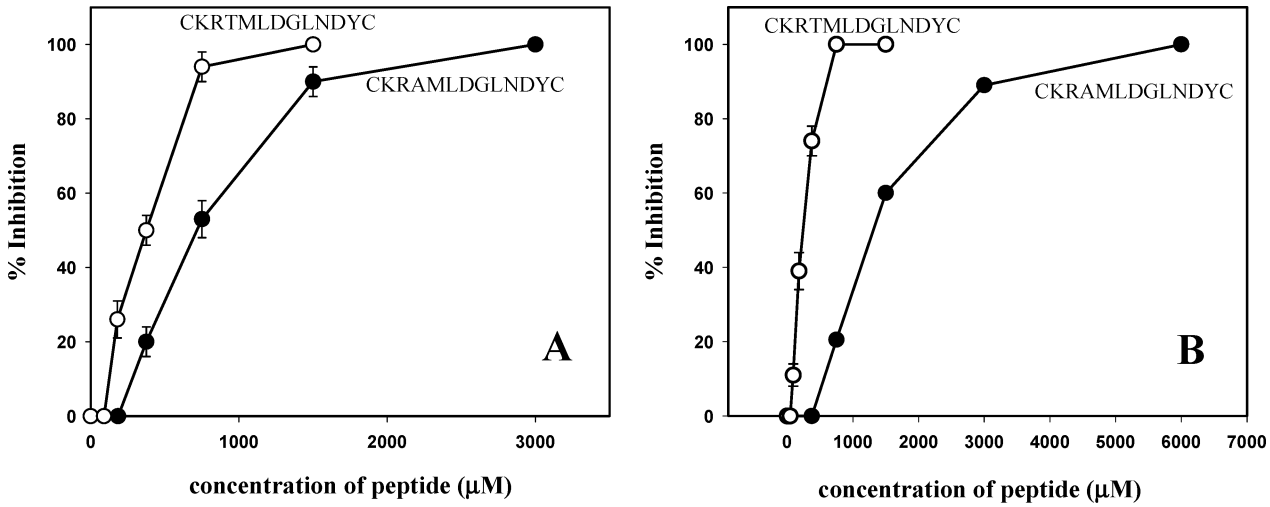

FIGURE 4: Effect of synthetic peptides, designed on the basis of the active site of VLO5 and EC3, on cell adhesion. The inhibitory effects of peptides CKRAMLDGLNDYC (filled circles) and CKRTMLDGLNDYC (open circles) were tested in an adhesion assay of CMFDA-labeled Jurkat cells (A) and α9SW480 cells (B) to immobilized VCAM-1. Different concentrations of peptides were incubated (30 min at 37 °C) with the cells (1×10^5) in the 96-well plate, previously covered with VCAM-1 (2 μg/mL), in 100 μL of HBSS containing calcium and magnesium. After being washed with the same buffer, the adhered cells were lysed by Triton X-100, and the plate was read using Cytofluor 2350. The percentage inhibition was calculated by comparison with fluorescence obtained from a control sample without disintegrins. The error bars represent the standard deviations in three independent experiments.

Table 1: Comparison of Inhibitory Effects of EC3 (*28*), VLO5, and EO5 on Various Integrins in Cell Adhesion Assay[a]

cell suspension	integrin	ligand	IC_{50} (nM) EC3	VLO5	EO5
α1K562	α1β1	Coll IV	>10000	>10000	>10000
α2K562	α2β1	Coll I	>10000	>10000	>10000
α6K562	α6β1	LM	>10000	>10000	>10000
K562	α5β1	FN	150	3400	690
Jurkat	α4β1	VCAM-1	16	5.5	9.5
Ramos	α4β1	VCAM-1	22	1.2	5.3
SW480α9	α9β1	VCAM-1	35	2.6	7.2
SW480α9	α9β1	OP	>10000	34	ND
SW480α9	α9β1	TN-C	>10000	29	ND
RPMI8866	α4β7	MAdCAM-1	17	185	120
A5	αIIbβ3	FG	500	760	980
JY	αvβ3	VN	>10000	>10000	>10000

[a] The data represent the mean of the results of three experiments. Abbreviations: Coll, collagen; LM, laminin; FN, fibronectin; VCAM-1, vascular cell adhesion molecule-1; OP, osteopontin (nOPNb RAA); TN-C, tenascin-C (TNfn3RAA); FG, fibrinogen; VN, vitronectin; α1,α2,α6K562, K562 cells transfected with α1, α2, or α6 integrins, SW480α9, SW480 cells transfected with α9 integrin, A5, CHO cells transfected with αIIbβ3 integrin; ND, non determined.

representing EC3 and VLO5 integrin-binding loops (Figure 4) confirmed data obtained for native disintegrins as inhibitors of human α4β1 and α9β1; the CKR*TMLD*GLNDYC peptide was more active in inhibition of both integrins than the CKR*AMLD*GNDYC peptide.

Interaction of MLD-Containing Disintegrins with Human and Mouse Melanoma Cell Lines. Human (HS.939T) and mouse (B16) melanoma cell lines express a panel of different β1 integrins (Figure 5A), including α4β1 integrin. Both types of cell lines adhered to immobilized EC3, VLO5, and EO5, and this adhesion was inhibited by blocking mAb's against α4 (Figure 5B) and β1 (Figure 5C) integrin subunits. The inhibitory effect of blocking anti-α5 mAb was partial for EC3 and negligible for VLO5 and EO5. The adhesion of mouse cells was more potent to EC3, whereas the human cell line much better adhered to VLO5 and EO5. This species selectivity of heterodimeric disintegrins was confirmed in an α4β1-dependent adhesion assay of HS.939T cells and B16 cells to human and mouse recombinant VCAM-1, respectively (Figure 6). The activity of VLO5 was over 1 order of magnitude higher than that of EC3 in inhibition of adhesion of the human cell line, whereas in the case of the mouse melanoma cell line, the reverse inhibitory effect was observed. The activity of EO5 was intermediate, but was closer to that of VLO5 than that of EC3.

DISCUSSION

In this study we compared the activities of three different heterodimeric disintegrins that lack an RGD motif. The RGD motif is the most commonly found motif in all disintegrin families, which inhibit platelet aggregation by blocking the fibrinogen receptor (*20*), as well as other so-called RGD-dependent integrins such as αvβ3 and α5β1 (*23*, *24*). EC3 is a non-RGD-containing heterodimeric disintegrin possessing both VGD and MLD motifs and is an inhibitor of α4β1 and α9β1 integrins (*34*, *35*). Two new disintegrins, VLO5 and EO5, structurally strictly related to EC3, were purified from the venoms of *V. lebetina obtusa* and *E. ocellatus*, respectively; in the first HPLC separation step of the whole venoms, these heterodimeric disintegrins were eluted at almost identical retention times (Figure 1). This confirmed the high homology of the molecular structures of these disintegrins. The retention times for RGD-containing, dimeric disintegrins were significantly different in this HPLC analysis. For example, homodimers CC5 (*33*) and VLO4 (*29*) displayed retention times of 21 and 22 min, respectively, whereas heterodimers CC8 (*33*), EC6 (*35*), and EMF10 (*31*) had retention times of 28, 29, and 26 min, respectively. It is interesting that under the same HPLC conditions each venom showed a characteristic elution pattern that could be treated as a "fingerprint" for each snake species. This analytical approach may be utilized as a method for analytical identification of species of venomous snakes, as it is both more rapid and more sensitive than immunological and electrophoretical procedures.

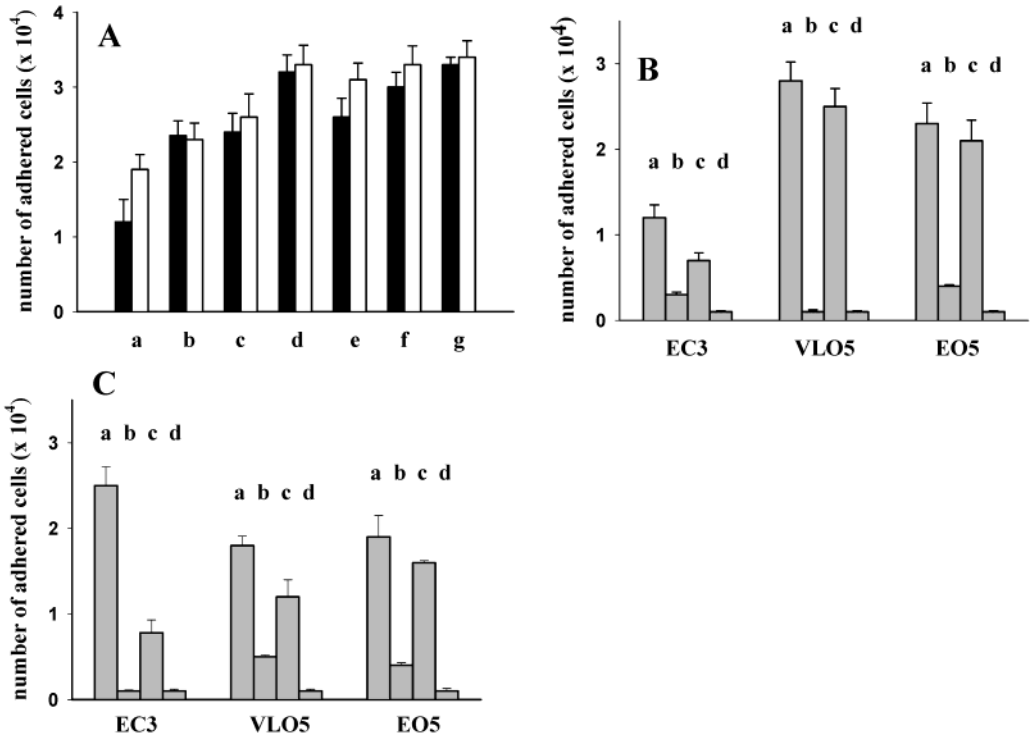

FIGURE 5: Interaction of MLD-containing disintegrins with human (HS.939T) and mouse (B16) melanoma cell lines. (A) Adhesion of HS.939T (filled bars) and B16 (open bars) to immobilized antibodies specific to various β1 integrins. The monoclonal antibodies (1 (μg/well)/100 μL of PBS) were immobilized overnight at 4 °C. After blocking, the CMFDA-labeled cells were added to each well in HBSS containing calcium and magnesium. After incubation for 30 min at 37 °C, unbound cells were washed out and bound cells were lysed using 0.5% Triton X-100. The number of adhered cells was calculated from the standard curve, prepared in parallel on the same plate from the known number of fluorescein-labeled cells. The mAb's were as follows: (a) anti-α1 mAb (AJH10 for human cells and Ha31/8 for mouse cells), (b) anti-α2 mAb (P1E6 for human cells and HMα2 for mouse cells), (c) anti-α3 mAb (P1B5 for human cells and clone 42 for mouse cells), (d) anti-α4 mAb (HP2/1 for human cells and R1-2 for mouse cells), (e) anti-α5 mAb (Sam-1 for human cells and HMα5-1 for mouse cells), (f) anti-α6 mAb (GoH3 for human and mouse cells), (g) anti-β1 maAb (Lia1/2 for human cells and Ha2/5 for mouse cells). (B) Effect of blocking mAb's (b) anti-α4 (HP2/1), (c) anti-α5 (Sam-1), and (d) anti-β1 (Lia1/2) on adhesion of HS.939T cells to immobilized disintegrins. (a) Control adhesion. (C) Effect of blocking mAb's (b) anti-α4 (R1-2), (c) anti-α5 (HMα5-1), and (d) anti-β1 (Ha2/5) on adhesion of B16 cells to immobilized disintegrins. (a) Control adhesion. The error bars represent standard deviations obtained from triplicate experiments.

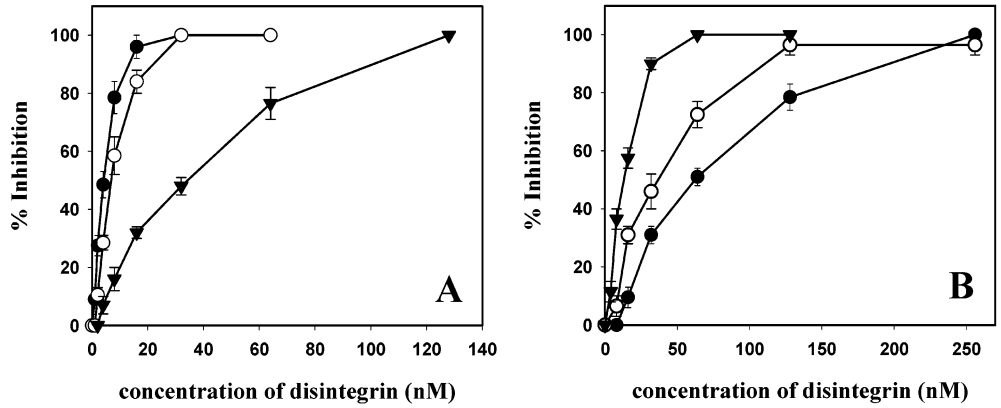

FIGURE 6: Effect of MLD-disintegrins on adhesion of HS.939T cells (A) and B16 cells (B) to VCAM-1. Human or mouse recombinant VCAM-1 (2 μg/mL) was immobilized on a 96-well plate, overnight at 4 °C in PBS. The increasing concentrations of EC3 (filled triangles), VLO5 (filled circles), or EO5 (open circles) were added to CMFDA-labeled cells, and the adhesion experiment was performed as described in the caption to Figure 5. The error bars represent standard deviations obtained from triplicate experiments.

The subunits of EC3, VLO5, and EO5 show a high degree of homology among themselves and other dimeric disintegrins. In particular, the VGD-integrin-binding loops of VLO5A and EO5B have identical sequence and differ in only one residue (M^{46}/V) from that of EC3A (Figure 2). On the other hand, the MLD-integrin-recognition loops of VLO5B and EO5A differ in one residue between themselves (R^{41}/K) and between them and EC3B (T^{42}/A). Although, the structure among the dimeric disintegrins is conserved, their inhibitory activities against various integrins are variable. This is especially striking in the case of the non-RGD-containing heterodimeric disintegrins. EC3, VLO5, and EO5 only poorly inhibit the two RGD-dependent integrins αIIbβ3 and α5β1, and their activity against a third RGD-dependent integrin, αvβ3, was absent even at a concentration of 10 μM (Table 1). On the other hand, the dimeric disintegrins

containing an RGD sequence are very potent inhibitors of α5β1 (*31*, *35*, *42*). EC3, VLO5, and EO5 are primarily inhibitors of the integrins α4β1, α4β7, and α9β1. All are receptors for VCAM-1, an adhesive molecule expressed on inflamed endothelium, which participates in leukocyte trafficking through the vessel wall. However, the three MLD-disintegrins showed different selectivity. VLO5 was a more potent inhibitor of α4β1 and α9β1 integrin interaction with VCAM-1 than EC3, whereas EC3 was a more potent inhibitor of α5β1 integrin binding to fibronectin and of α4β7 binding to MAdCAM-1. Moreover, EC3 did not inhibit the adhesion of α9-expressing cells to osteopontin and tenascin-C up to a concentration 10 μM, whereas VLO5 blocked this interaction with IC_{50} values of 34 and 29 nM, respectively. These data indicate that the integrin-binding loop of VLO5 is structurally formed to bind with a higher affinity to human VLA-4 and VLA-9. Conversely, the structure of EC3 interacts preferentially with the α4β7 integrin.

The activities of synthetic peptides representing the MLD-loops of EC3 and VLO5 support the hypothesis that amino acids surrounding the active motif of the disintegrin determine their selective interaction with specific integrins (Figure 4). These results are in line with previous work on monomeric disintegrins and synthetic peptides showing that amino acids surrounding the RGD tripeptide motif are important for conferring selectivity and potency toward integrins. Hence, RGDN-containing disintegrins were greater than 10-fold more potent than RGDW-containing disintegrins in blocking the adhesion of cells mediated by α5β1 (*43*), whereas the presence of an aromatic residue C-terminal to the RGD sequence, such as phenylalanine (F) or tryptophan (W), enhances severalfold the ability of the disintegrins to inhibit platelet aggregation and binding of fibrinogen to purified αIIbβ3 (*44*). NMR studies on cyclic RGD peptides (*45*) provided a structural ground to the concept that the amino acid residue adjacent to the C-terminal end of the RGD motif modulates the shape of the integrin-binding loop and that different integrins distinguish the conformational environment of various RGD sites (*23*, *24*, *27*, *46*). These studies have strengthened the importance of the C-terminally adjacent amino acid to the RGD sequence in the modulation of the integrin inhibition characteristic for monomeric, RGD-containing disintegrins. Our results with VLO5, EO5, and EC3 are the first to show that the residue N-terminally flanking the MLD motif also contributes to the integrin-binding selectivity and potency.

In this study we successfully applied a new purification method of α4β1 and α9β1 integrins. The heterodimeric disintegrin VLO5 was used as a ligand coupled to the resin for affinity chromatography. For detachment of bound integrin, we used only EDTA instead of low pH conditions normally required for recovery of integrin coupled to an antibody column. Both purified integrins bound potently to immobilized ligands (VCAM-1, MLD-disintegrins) in the ELISA assay (data not shown). Moreover, after immobilization on the plate, α4β1 and α9β1 interacted with soluble VCAM-1, and this interaction was inhibited by MLD-disintegrins (Figure 3); the inhibitory effect was the most potent for VLO5 and less for EC3, confirming the data we obtained in the adhesion studies.

Among the MLD-disintegrins we also observed interspecies selectivity; similar selectivity has been previously observed for RGD-disintegrins (*47*, *48*). We compared the ability of all three non-RGD-containing disintegrins to interact with human and mouse α4β1 integrin in an adhesion assay. The data presented in Figures 5 and 6 clearly indicated very high potency of VLO5 and EO5 in interacting with human integrin, whereas EC3 was more selective for murine α4β1. This observation indicates that the configuration of the ligand-binding site in this integrin appears to differ in human and mouse cells. MLD-disintegrins appear to be useful probes for comparing the spatial requirements of human and mouse α4β1 for interaction with their ligands. The preferential interaction of the disintegrin containing the TMLD motif in the putative integrin-binding loop with human integrin and the AMLD motif with murine integrin could be important in the therapeutic design of low molecular weight inhibitors of α4β1. Currently, many laboratories are searching α4β1 integrin blockers for potential application in the treatment of autoimmune and inflammatory diseases (*49*). The potential species selectivity of peptides blocking α4β1 is an important issue in the interpretation preclinical data.

ACKNOWLEDGMENT

This work was supported by an American Heart Association Beginning Investigator grant (C.M.) and by Grant BMC2001-3337 from the Dirección General de Enseñanza Superior e Investigación Científica, Madrid, Spain (J.J.C.).

REFERENCES

1. Hynes, R. O. (1992) *Cell 69*, 11−25.
2. Ruoslahti, E. (1996) *Annu. Rev. Cell Dev. Biol. 12*, 697−715.
3. Sheppard, D. (2000) *Matrix Biol. 19*, 203−209.
4. Hynes, R. O. (2002) *Cell 110*, 673−687.
5. Liddington, R. C., and Ginsberg, M. H. (2002) *J. Cell Biol. 158*, 833−839.
6. Takagi, J., Petre, B. M., Walz, T., and Springer, T. A. (2002) *Cell 110*, 599−611.
7. Arnaout, M. A. (2002) *Immunol. Rev. 186*, 125−140.
8. Brakebusch, C., and Fässler, R. (2002) *EMBO J. 22*, 2324−2333.
9. McMurray, R. W. (1996) *Semin. Arthritis Rheum. 25*, 215−233.
10. Oppenheimer-Marks, N., and Lipsky, P. E. (1996) *Clin. Immunol. Immunopathol. 79*, 203−210.
11. Clements, J. M., Newham, P., Shepherd, M., Gilbert, R., Dudgeon, T. J., Needham, L. A., Edwards, R. M., Berry, L., Brass, A., and Humphries, M. J. (1994) *J. Cell Sci. 107*, 2127−2135.
12. Taooka, Y., Chen, J., Yednock, T., and Sheppard, D. (1999) *J. Cell Biol. 145*, 413−420.
13. Wayner, E. A., and Kovach, N. L. (1992) *J. Cell Biol. 116*, 489−497.
14. Newman, P., Craig, S. E., Seddon, G. N., Schofield, N. R., Rees, A., Edwards, R. M., Jones, E. Y., and Humphries, M. J. (1997) *J. Biol. Chem. 272*, 19429−19440.
15. Yokosaki, Y., Palmer, E. L., Prieto, A. L., Crossin, K. L., Bourdon, M. A., Pytela, R., and Sheppard, D. (1994) *J. Biol. Chem. 269*, 26691−26696.
16. Smith, L. L., Cheung, H. K., Ling, L. E., Chen, J., Sheppard, D., Pytela, R., and Giachelli, M. C. *J. Biol. Chem. 271*, 28485−28491.
17. Yokosaki, Y., Matsuura, N., Higashiyama, S., Murakami, I., Obara, M., Yamakido, M., Shigeto, N., Chen, J., and Sheppard, D. (1998) *J. Biol. Chem. 273*, 11423−11428.
18. Yokosaki, Y., Matsuura, N., Sasaki, T., Murakami, I., Schneider, H., Higashiyama, S., Saitoh, Y., Yamakido, M., Taooka, Y., and Sheppard, D. (1999) *J. Biol. Chem. 274*, 36328−36334.
19. Dennis, M. S., Henzel, W. J., Pitti, R. M., Lipari, M. T., Napier, M. A., Deisher, T. A., Bunting, S., and Lazarus, R. A. (1990) *Proc. Natl. Acad. Sci. U.S.A. 87*, 2471−2475.
20. Niewiarowski, S., McLane, M. A., Kloczewiak, M., and Stewart, G. J. (1994) *Semin. Hematol. 31*, 289−300.

21. McLane, M. A., Marcinkiewicz, C., Vijay-Kumar, S., Wierzbicka-Patynowski, I., and Niewiarowski, S. (1998) *Proc. Soc. Exp. Biol. Med. 219*, 109−119.
22. Calvete, J. J., Jurgens, M., Marcinkiewicz, C., Romero, A., Schradere, M., and Niewiarowski, S. (2000) *Biochem. J. 345*, 573−581.
23. Marcinkiewicz, C., Senadhi, V. K., McLane, M. A., and Niewiarowski, S. (1997) *Blood 90*, 1565−1575.
24. Wierzbicka-Patynowski, I., Niewiarowski, S., Marcinkiewicz, C., Calvete, J. J., Marcinkiewicz, M. M., and McLane, M. A. (1999) *J. Biol. Chem. 274*, 37809−37814.
25. Scarborough, R. M., Rose, J. W., Hsu, M. A., Phillips, D. R., Fried, V. A., Campbell, A. M., Nannizzi, L., and Charo, I. F. (1991) *J. Biol. Chem. 266*, 9359−9362.
26. Oshikawa, K., and Terada, S. (1999) *J. Biochem. 125*, 31−35. Lu, X., Rahman, S., Kakkar, V. V. and Authi, K. S. (1996) *J. Biol. Chem. 271*, 289−294.
27. Shimokawa, K.-I., Jia, L.-G., Shannon, J. D., and Fox, J. W. (1998) *Arch. Biochem. Biophys. 354*, 239−246.
28. Lu, X., Rahman, S., Kakkar, V. V., and Authi, K. S. (1996) *J. Biol. Chem. 271*, 289−294.
29. Calvete, J. J., Moreno-Murciano, M. P., Theakston, R. D. G., Kisiel, D. G., and Marcinkiewicz, C. (2003) *Biochem. J. 372*, 725−734.
30. Gsami, A., Srairi, N., Guermazi, S., Dkhil, H., Karoui, H., and El Ayeb, M. (2001) *Biochim. Biophys. Acta 1547*, 51−56.
31. Marcinkiewicz, C., Calvete, J. J., Vijay-Kumar, S., Marcinkiewicz, M. M., Raida, M., Schick, P., Lobb, R. R., and Niewiarowski, S. (1999) *Biochemistry 38*, 13302−13309.
32. Nikai, T., Taniguchi, K., Komori, Y., Masuda, K., Fox, J. W., and Sugihara, H. (2000) *Arch. Biochem. Biophys. 378*, 6−15.
33. Calvete, J. J., Fox, J. W., Agelan, A., Niewiarowski, S., and Marcinkiewicz, C. (2002) *Biochemistry 41*, 2014−2021
34. Marcinkiewicz, C., Calvete, J. J., Marcinkiewicz, M. M., Raida, M., Vijay-Kumar, S., Huang, Z., Lobb, R. R., and Niewiarowski, S. (1999) *J. Biol. Chem. 274*, 12468−12473.
35. Marcinkiewicz, C., Taooka, Y., Yokosaki, Y., Calvete, J. J., Marcinkiewicz, M. M., Lobb, R. R., Niewiarowski, S., and Sheppard, D. (2000) *J. Biol. Chem. 275*, 31930−31937.
36. Brando, C., Marcinkiewicz, C., Goldman, B., McLane, M. A., and Niewiarowski, S. (1999) *Biochim. Biophys. Res. Commun. 267*, 413−417.
37. Wang, A., Yokosaki, Y., Ferrand, R., Balmas, J., and Sheppard, D. (1996) *Am. J. Respir. Cell Mol. Biol. 15*, 664−672.
38. Gotwals, P. J., Chi-Rosso, G., Ryan, S. T., Sizing, I., Zafari, M., Benjamin, C., Singh, J., Venyaminov, S. Y., Pepinsky, R. B., and Koteliansky, V. (1999) *Biochemistry 38*, 8280−8288.
39. Smith, J. B., Theackston, R. D. G., Coelho, A. L., Barja-Fidalgo, C., Calvete, J. J., and Marcinkiewicz, C. (2002) *FEBS Lett. 512*, 111−115.
40. O'Toole, T. E., Loftus, J. C., Du, X., Glass, A., Ruggeri, Z. M., Shattil, S. J., Plow, E. F., and Ginsberg, M. H. (1990) *Cell Regul. 1*, 883−893.
41. Marcinkiewicz, C., Rosenthal, L. A., Marcinkiewicz, M. M., Kowalska, M. A., and Niewiarowski, S. (1996) *Protein Expr. Purif. 8*, 68−74.
42. Zhou, Q., Nakada, M. T., Brooks, P. C., Swenson, S. D., Ritter, M. R., Argounova, S., Arnold, C., and Markland, F. S. (2000) *Biochem. Biophys. Res. Commun. 267*, 350−355.
43. Scarborough, R. M., Rose, J. W., Naughton, M. A., Phillips, D. R., Nannizzi, L., Arfsten, A., Campbell, A, M., and Charo, I. F. (1993) *J. Biol. Chem. 268*, 1058−1065.
44. McLane, M. A., Kowalska, M. A., Silver, L., Shattil, S. J., and Niewiarowski, S. (1994) *Biochem. J. 301*, 429−436.
45. Pfaff, M., Tangemann, K., Müller, B., Gurrath, M., Müller, G., Kessler, H., Timpl, R., and Engel, J. (1994) *J. Biol. Chem. 269*, 20233−20238.
46. McLane, M. A., Senadhi, V. K., Marcinkiewicz, C., Calvete, J. J., and Niewiarowski, S. (1996) *FEBS Lett. 391*, 139−143.
47. Lombardi, P., Pelagalli, A., Avallone, L., d'Angelo, D., Belisario, M. A., d'Angelo, A., and Staiano, N. (1999) *J. Comput. Pathol. 121*, 185−190.
48. Chen, Y. L., Huang, T. F., Chen, S. W., and Tsai, I. H. (1995) *Biochem. J. 305*, 513−520.
49. Jackson, D. Y. (2002) *Curr. Pharm. Des. 8*, 1229−1253.

BI035853T